

## 특수 설계된 마찰교반도구(Friction Stir Process Tool)를 사용한 HDPE 나노복합체 제조방법

B. Balamugundan<sup>\*†</sup>, L. Karthikeyan<sup>\*\*\*</sup>, and M. Puviyarasan<sup>\*\*</sup>

<sup>\*</sup>Department of Mechanical Engineering, Sathyabama University

<sup>\*\*</sup>Department of Mechanical Engineering, Panimalar Engineering College  
(2017년 5월 5일 접수, 2017년 7월 28일 수정, 2017년 8월 18일 채택)

## Feasibility of Fabricating HDPE Nanocomposites Using a Specially Designed Friction Stir Process Tooling System

B. Balamugundan<sup>\*†</sup>, L. Karthikeyan<sup>\*\*\*</sup>, and M. Puviyarasan<sup>\*\*</sup>

<sup>\*</sup>Department of Mechanical Engineering, Sathyabama University, Chennai-119, India

<sup>\*\*</sup>Department of Mechanical Engineering, Panimalar Engineering College, Chennai-123, India

(Received May 5, 2017; Revised July 28, 2017; Accepted August 18, 2017)

**Abstract:** Polymer nanocomposites are being increasingly used in a variety of tribological applications owing to their structural features. In this study, high density polyethylene (HDPE) composites with three different nanoparticles such as alumina ( $\text{Al}_2\text{O}_3$ ), multi-walled carbon nanotubes (MWCNT) and graphene were fabricated using a newly designed friction stir processing tool and fixture. Mechanical test results showed that the fabricated polymer nanocomposites possess enhanced mechanical properties at higher tool rotational speed and traverse feed. The frictional coefficient and wear properties of the fabricated polymer nanocomposites were evaluated under dry sliding conditions using a pin-on-disc tribometer. Further the surfaces of the fabricated samples before and after wear studies were evaluated using scanning electron microscope. The wear test results showed that the HDPE/MWCNT has a very low mass loss as compared with HDPE/graphene, HDPE/ $\text{Al}_2\text{O}_3$  composites and HDPE parent material. Moreover MWCNT particles act as a lubricant during wear test causing the worn surface of HDPE/MWCNT nanocomposites to be smoother as compared to other fabricated nanocomposites. The higher reflection peak between  $23.71^\circ$  to  $23.95^\circ$  obtained using X-ray diffraction (XRD) for the HDPE nanocomposites fabricated with the nanoparticles MWCNT,  $\text{Al}_2\text{O}_3$  and graphene reveal a uniform mixture of the polymer matrix with the nanoparticles. The XRD results also show that the addition of nanoparticles does not significantly alter the crystal structure of the HDPE matrix.

**Keywords:** friction stir processing, high density polyethylene, graphene, multi-walled carbon nanotubes, alumina.

### Introduction

Among the many available polymers high density polyethylene (HDPE) is the third largest thermoplastic used worldwide with numerous applications. They are highly durable, chemically non reactive, inexpensive and easy to process.<sup>1</sup> However its lower tensile strength makes it unsuitable for heavy duty applications.<sup>2</sup> To increase the strength of the polymers they are normally reinforced with nano and micro par-

ticles. The reinforced polymer nanocomposites are increasingly being used in various assemblies and equipments including gear, bearings, joints, seals, food conveyors, semiconductors, automobile elements owing to their light weight, flexibility, excellent corrosion resistance, good processability and low cost.<sup>3-11</sup> Several techniques such as vacuum arc deposition, melt mixing and injection molding are being used to fabricate the polymer matrix composites (PMC) by mixing polymer matrix and nanoparticles under high temperature.<sup>12-18</sup>

Chee *et al.*<sup>19</sup> used 'melt mixing' technique to fabricate low density polyethylene composites with nano  $\text{Al}_2\text{O}_3$  reinforcements at  $125^\circ\text{C}$ . Silane was used as a coupling agent to enhance the interfacial interactions between alumina and low

<sup>†</sup>To whom correspondence should be addressed.  
E-mail: bala757609@gmail.com

©2018 The Polymer Society of Korea. All rights reserved.

density polyethylene. The results showed that among the various weight percentage proportions used, 1wt% nano-alumina successfully enhanced the mechanical properties of low density polyethylene material.

Sengupta *et al.*<sup>20</sup> observed an enhancement in mechanical and electrical properties of graphene reinforced HDPE nanocomposites. Bhattacharyya *et al.*<sup>21</sup> used prereluction and *in-situ* method to disperse graphene particles into ultra high molecular weight polyethylene for the fabrication of nanocomposite films. The nanocomposite film produced by prereluction method was found to possess higher crystalline characteristics, better modulus, strength, network hardening and creep resistance as compared to the '*in situ*' method. Lin *et al.*<sup>22</sup> used 'melt blending' technique to fabricate polyethylene/graphene oxide nanocomposites. The experimental results showed an increase of 20 and 13% in Young's modulus and tensile strength respectively. Achaby and Quaiss<sup>23</sup> prepared HDPE/graphene nano sheets and HDPE/MWCNT nanocomposites with equal weight percentage using melt mixing technique. The result showed that HDPE/graphene nanocomposites with higher specific surface area exhibit better mechanical properties as compared to HDPE/MWCNTs nanocomposites. Behrouz *et al.*<sup>24</sup> developed a coarse grained model to capture the interactions between polymer chains and nanotubes. It was found that the mechanical properties of the nanocomposites can be estimated with higher accuracy and lower computational cost using coarse grained model simulation.

Recently, friction stir processing (FSP) a novel solid state processing technique has gained wide acceptance in fabricating polymer matrix composites. Composites fabricated by FSP were found to possess an inner matrix with better ductility and toughness and an outer surface with improved wear resistance and strength.<sup>1</sup> During friction stir processing the tool pin serves two primary functions: (a) heating of work piece and (b) movement of material. The friction between the tool and the work piece develops heat which softens the material around the rotating pin. The rotation also causes material movement from the advancing to the retreating side of the pin. The tool shoulder consolidates the material that flows around the pin.<sup>25</sup> Puviyarasan and Senthil Kumar<sup>26,27</sup> fabricated aluminum AA6061/B<sub>4</sub>C and AA6061/SiC<sub>p</sub> metal matrix composites through friction stir processing and found that higher tensile strength and microhardness was achieved in the composites fabricated using optimum process parameters. Hosseini *et al.*<sup>28</sup> have observed a microstructural modification, grain size reduction and homogeneous distribution of reinforcements in alu-

minum Al5083 grade using friction stir processing method.

Prakash *et al.*<sup>29</sup> used FSP technique to develop alumina/0.5 graphene reinforced AA6061 hybrid composite sheets with higher hardness and minimum wear rate. Yet fabricating PMCs through conventional FSP tool is highly difficult owing to the differences in the material structure, morphology of the matrix, low melting temperature, low thermal conductivity, microhardness and short solidification time.<sup>30-32</sup> In order to avoid these defects Rezgui *et al.*<sup>33</sup> developed a new FSP tooling system that utilizes a stationary wooden shoulder to lap weld HDPE sheets. However the poor thermal conductivity of wood caused the formation of a small sized HAZ and discontinuities in the weld. Barmouz *et al.*<sup>1</sup> fabricated HDPE/clay nanocomposites using FSP and studied the effect of process parameters on its morphology and mechanical properties.

Azarsa and Mostafapour<sup>34</sup> fabricated HDPE/copper powder polymer metal matrix composites using a FSP tool with stationary shoulder and a heater. The results showed that the ultimate tensile strength and elastic modulus of the fabricated composites were remarkably enhanced. Yet studies conducted on the fabrication of PMCs through FSP using a stationary shoulder are negligible.

In this work an attempt has been made to develop and apply a novel FSP tooling system using a stationary shoulder without any external heat source to fabricate HDPE/Al<sub>2</sub>O<sub>3</sub>, HDPE/MWCNTs and HDPE/graphene nanocomposites. The tensile strength and tribological behavior of the fabricated composites were evaluated. Microstructural analysis using scanning electron microscopy (SEM) and XRD was carried out to confirm the dispersion of nanoparticles in the HDPE without any prominent defects.

## Experimental

A high density polyethylene copolymer of HDPE5218EA grade with good flowability, narrow volume distribution, suitable for thin wall injection molding was used as matrix. The as-received materials were cut into rectangular plates with the dimensions 200×200×10 mm. Al<sub>2</sub>O<sub>3</sub>, MWCNT and graphene nanoparticles with a particle size of 20 nm and 99.9% purity were used as particulate reinforcements.

Fabrication of PMCs through FSP requires a novel FSP tooling and fixture system as the material structure and thermal conductivity of polymers are different as compared to the metals. The designed FSP tool consists of a thrust bearing, cylindrical rotating pin and a stationary shoulder. During friction stir

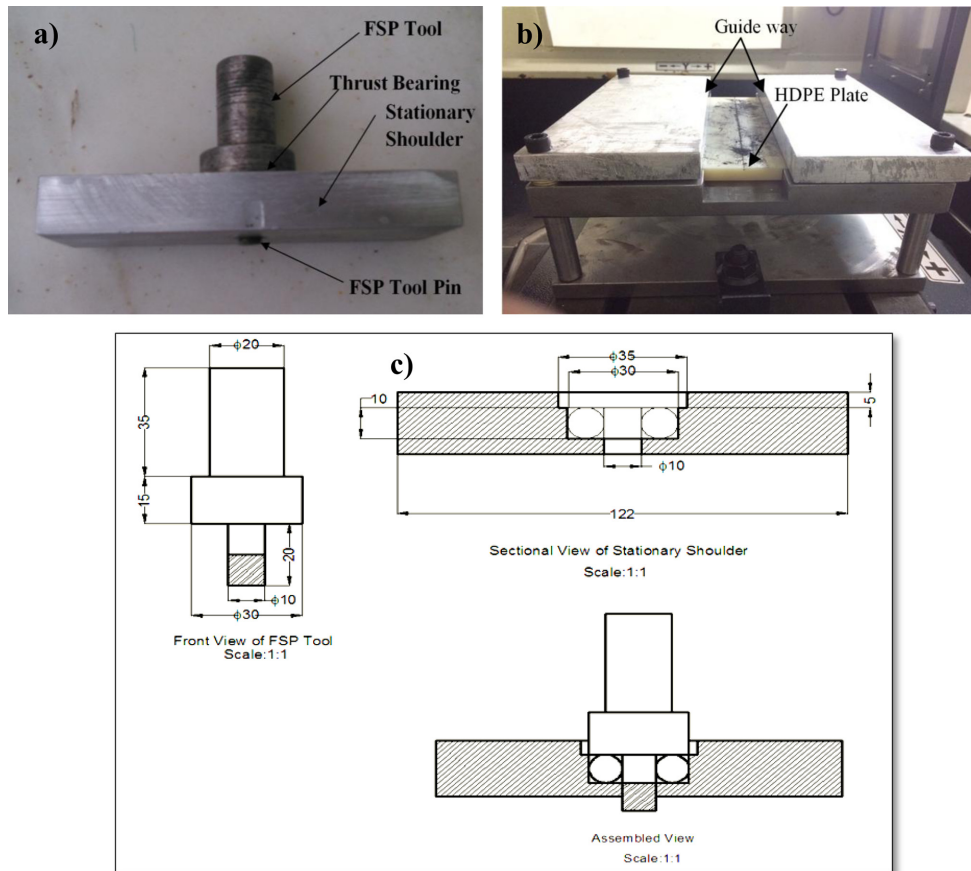


**Figure 1.** (a) FSP tool with stationary shoulder; (b) fixture; (c) dimensions of the designed FSP tool.

processing, the thrust bearing separates the shoulder from the FSP tool pin and keeps it stationary relative to the pin. Tool steel of H13 grade with 1 mm pitch, hardened to HRC56 was used to fabricate the thread pin. The stationary shoulder was fabricated using AA6061 aluminum alloy, chosen for its superior strength and higher thermal conductivity. The polymer plate was located inside a slot cut in the fixture. A guide way was provided for the stationary shoulder at the top of the fixture. Figure 1 shows the designed tooling system.

In order to fabricate HDPE/ $\text{Al}_2\text{O}_3$ , HDPE/MWCNTs and HDPE/graphene polymer nanocomposites, initially  $\text{Al}_2\text{O}_3$ , MWCNT and graphene particles were filled into a groove of 1 mm width and 2 mm depth, cut separately in the middle of the matrix. Based on the relation given in eq. (1)<sup>35</sup> the volume fraction of  $\text{Al}_2\text{O}_3$ , MWCNT and graphene particles was calculated as 15%.

$$\text{Volume fraction} = \frac{\text{Area of compaction/Groove}}{\text{Area of pin swept}} \quad (1)$$

During FSP the tool pin was inserted into the polymer

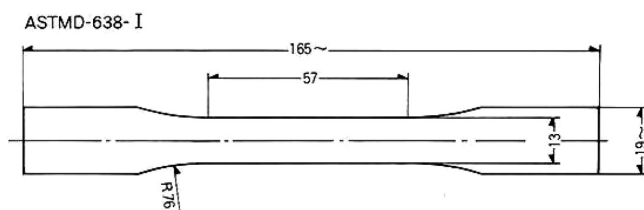
matrix till the stationary shoulder touches the upper surface of the polymer. This tooling system with stationary shoulder renders the 'FSP tool without pin' commonly used during the first run of the fabrication of composites unnecessary. Moreover, the stationary shoulder allows for a uniform cooling rate which provides the required additional heat.<sup>34</sup> In this study, only single stir passes were used. The values of process parameters used in this study are listed in Table 1. The process parameters were selected based on the previous studies.<sup>34</sup>

Tensile and wear tests were conducted for the fabricated polymer nanocomposites. The tensile test specimens were extracted from the fabricated polymer nanocomposites along the longitudinal direction as per ASTM D638-Type I standards using water jet machining. Tensile tests were carried out at room temperature using a computerized universal testing machine with a loading rate of 50 mm/min and maximum force of 5 kN. The configuration and size of the extracted tensile specimen is shown in Figure 2.

The microhardness of the fabricated nanocomposites was measured using a standard Vickers microhardness tester along

**Table 1. Process Parameters Used in This Investigation**

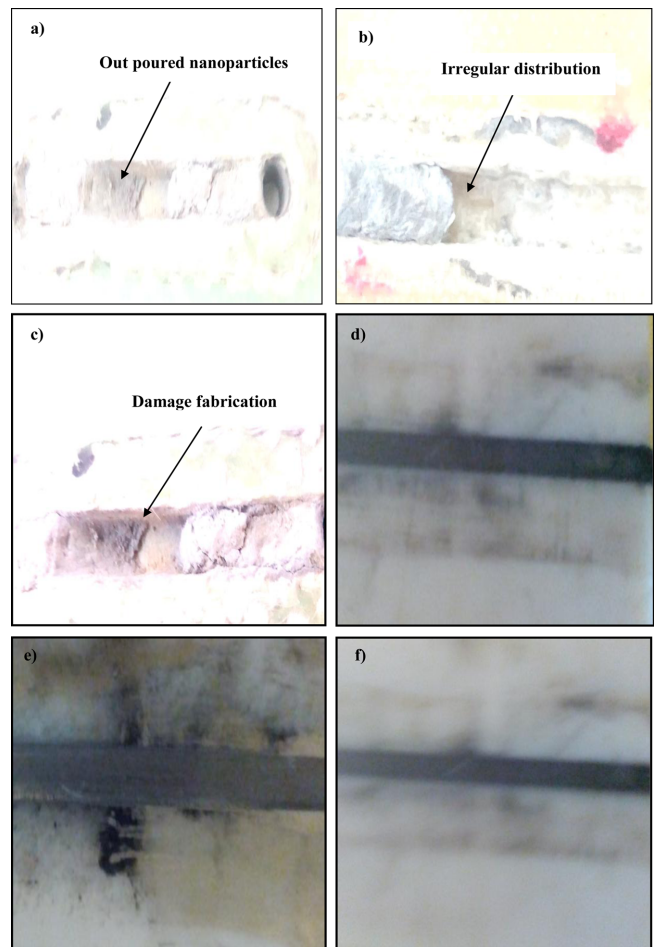
Sample	Rotational speed (rpm)	Traverse feed (mm/min)	Nanoparticles
S1	800	10	Al <sub>2</sub> O <sub>3</sub>
S2	800	10	MWCNT
S3	800	10	Graphene
S4	1000	15	Al <sub>2</sub> O <sub>3</sub>
S5	1000	15	MWCNT
S6	1000	15	Graphene
S7	Pure HDPE without nanoparticles		

**Figure 2.** Configuration and size of the tensile test specimen.

the processing direction by applying a load of 100 g for 10 s. An infrared thermometer having a temperature range from -35 to 800 °C was used to measure the temperature on the surface of the stationary shoulder. The microstructure of the fabricated composites was analyzed using a scanning electron microscope. Dry sliding wear test was conducted using a pin on disc machine according to ASTM G99 standards for polymeric samples. The prepared wear test samples were placed tightly inside the holder with screws perpendicular to the rotating disc. Wear load was applied using a lever attachment. The wear parameters such as time of rotational speed in rpm, track diameter and the desired load were fixed manually prior to each experiment.

## Results and Discussion

**Mechanical Properties.** Figure 3 shows the nanocomposites fabricated through conventional FSP technique and stationary shoulder FSP technique. It can be observed that the HDPE/Al<sub>2</sub>O<sub>3</sub>, HDPE/MWCNT and HDPE/graphene composites were successfully fabricated using the stationary shoulder technique. On the other hand the same polymer composites fabricated using conventional FSP technique under same process parameters displayed huge defects. Table 2 shows the mechanical properties of nanocomposites fabricated using stationary shoulder FSP technique. The mechanical properties of

**Figure 3.** Picture of fabricated samples using (a-c) conventional FSP; (d-f) stationary shoulder.

all the fabricated nanocomposites were found to be higher under the process parameters of 1000 rpm tool rotational speed and 15 mm/min traverse feed. At lower tool rotational speed and traverse feed the temperature developed in the stationary shoulder was insufficient to evenly distribute nanocomposites within HDPE matrix. With increasing tool rotational speed and traverse feed the temperature experienced in the stationary shoulder was also high (98 °C  $\approx$  0.8  $T_m$ ). This led to a better dispersion and higher level of interfacial adhesion between the nanoparticles and polymer matrix thereby significantly enhancing its mechanical properties such as ultimate tensile strength, yield strength and percentage elongation. The fabrication of defect free nanocomposites using stationary shoulder FSP technique confirms its higher efficiency as compared to conventional FSP technique.

The variation in ultimate tensile strength, yield strength and percentage elongation for the fabricated HDPE/Al<sub>2</sub>O<sub>3</sub>, HDPE/

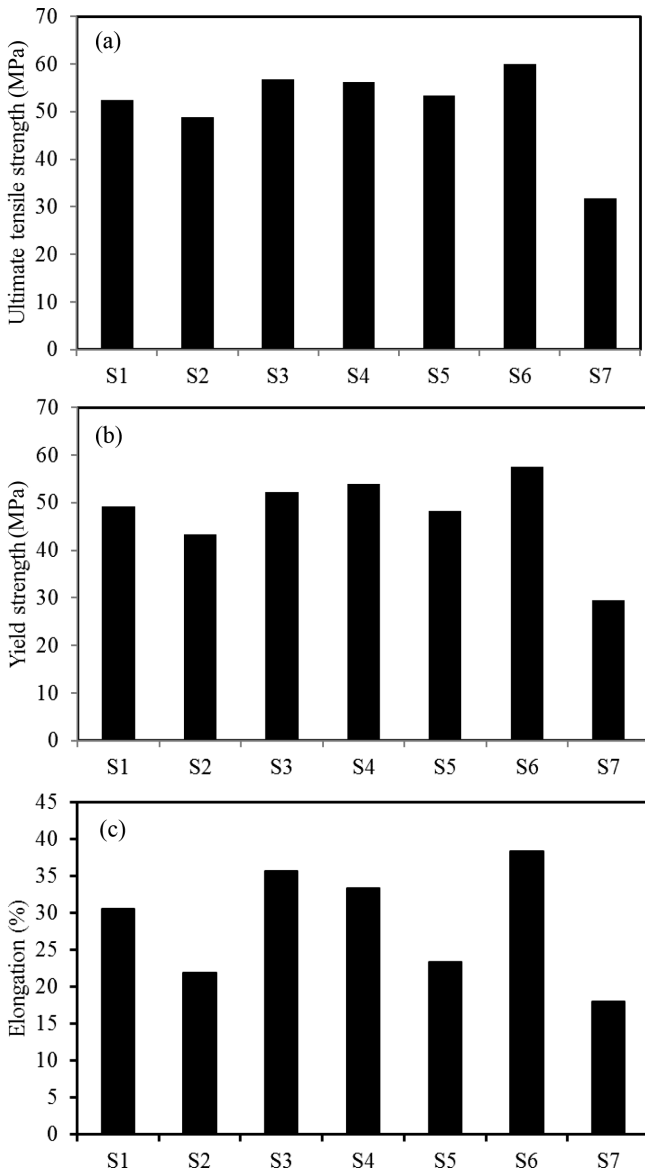


**Figure 4.** Variation in mechanical properties of fabricated samples. (a) ultimate tensile strength; (b) yield strength; (c) percentage elongation.

MWCNT and HDPE/graphene polymer nanocomposites is shown in Figure 4(a-c). The results show that HDPE/graphene has higher mechanical properties as compared to the HDPE/MWCNT and HDPE/Al<sub>2</sub>O<sub>3</sub> nanocomposites.

**Stress Strain Graph.** Figures 5 and 6 show the stress strain curves of HDPE/Al<sub>2</sub>O<sub>3</sub>, HDPE/MWCNT and HDPE/graphene under various friction stir processed parameters. It can be observed that the ultimate tensile strength, yield strength and percentage elongation of graphene reinforced HDPE nanocomposites were higher than the other nanoparticles reinforced

**Table 2. Mechanical Properties of Fabricated Nanocomposites**

Sample number	Tensile strength (MPa)	Yield strength (MPa)	Elongation (%)
S1	52.456	49.286	30.52
S2	48.785	43.33	21.85
S3	56.825	52.25	35.63
S4	56.275	54.01	33.33
S5	53.405	48.23	23.33
S6	60.013	57.48	38.33
S7	31.753	29.54	18

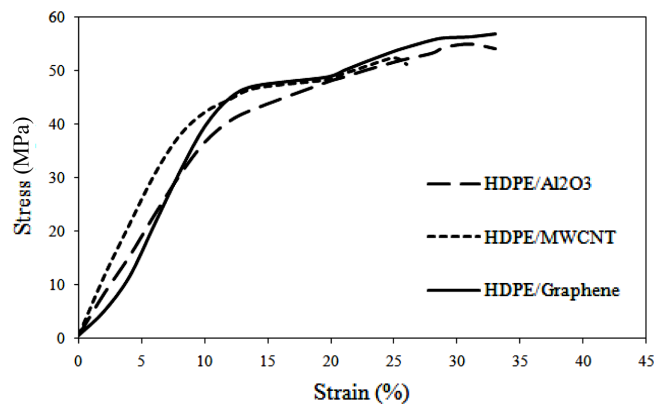


**Figure 5.** Stress-strain curve of HDPE/nanocomposites at 800 rpm and 10 mm/min.

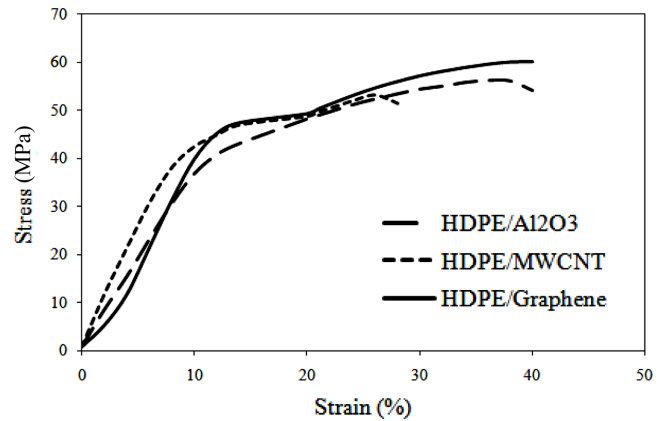


**Figure 6.** Stress-strain curve of HDPE/nanocomposites at 1000 rpm and 15mm/min.

composites. Though graphene and MWCNT particles have similar values of strength and Young's modulus, the two-dimensional graphene acts as an effective strengthening and toughening agent as compared to the 1-dimensional MWCNT.<sup>36-38</sup> Moreover graphene increases the plasticity of the fabricated nanocomposites. This results in the enhancement

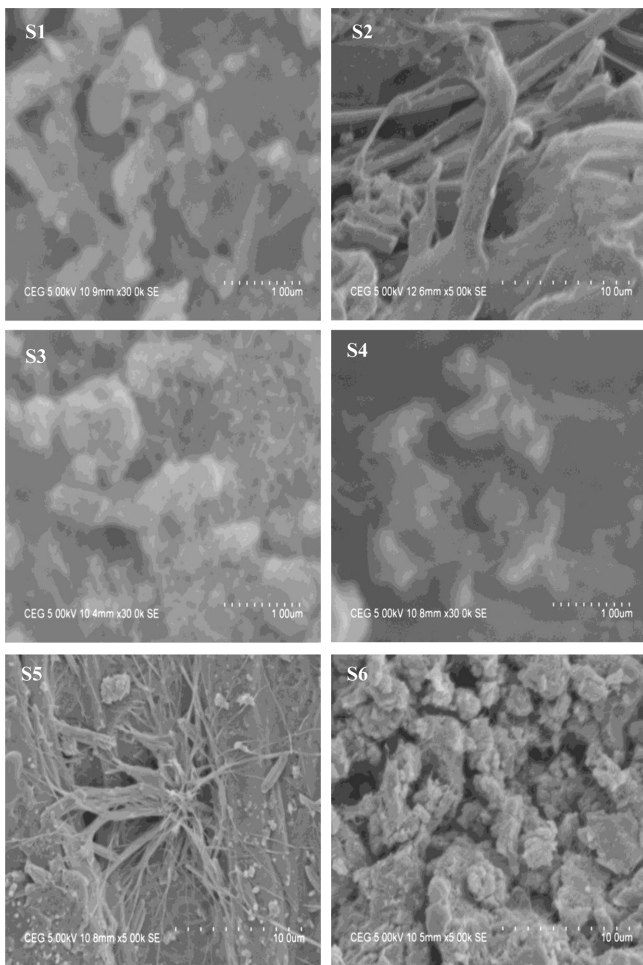


**Figure 7.** SEM images of fabricated HDPE/nanocomposites S1-S6.

of mechanical properties in graphene reinforced nanocomposites.

**Micro Structural Evaluation of Nanoparticle Distribution.** The SEM images of the fabricated samples under different process conditions are shown in Figure 7. It is well known that polymers such as HDPE are soft in nature and the introduction of nanoparticles such as  $\text{Al}_2\text{O}_3$ , MWCNT and graphene will enhance its ultimate tensile strength, yield strength, percentage elongation, microhardness and wear resistance.

The microstructural images of the nanocomposites fabricated through friction stir processing shows a uniform distribution of nanoparticles within the HDPE matrix (Figure 7). This can be attributed to the better stirring action of pin, uniform distribution of the heat generated by the stationary shoulder and adequate pressure of designed tooling system on the processed zone. In this work the temperature developed at the stationary shoulder under a rotational speed of 800 rpm was 75 °C ( $0.6 T_m$  of HDPE) and 1000 rpm was 98 °C ( $0.8 T_m$  of HDPE). Since no external heat was supplied to the stationary shoulder, the developed temperature was evenly distributed to the advancing and retreating sides of the processed region by the designed FSP tooling with stationary shoulder system. This results in a homogeneous distribution of reinforcement particles within the matrix. The cross sectional area of the processed zone is shown in the Figure 8.

Generally lower stationary shoulder temperature and higher traverse feed leads to the formation of large voids inside the

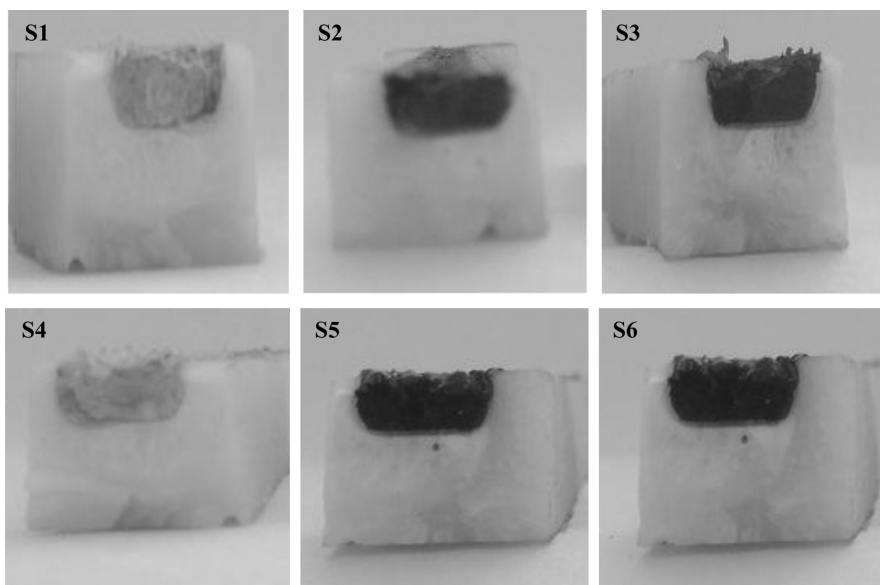


**Figure 8.** Cross section images of fabricated samples S1-S6.

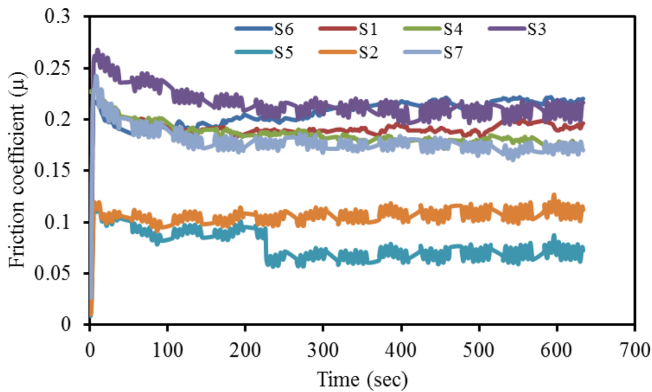


**Figure 9.** Friction coefficient of fabricated samples with respect to time.

stir zone which will significantly affect the mechanical properties. In this work the even distribution of temperature over the advancing and retreating sides of the tool shoulder is evident from the absence of the voids.

**Tribological Behavior of Fabricated Polymer Nanocomposites.** The room temperature friction and wear tests were carried out using a pin-on-disc apparatus under dry sliding conditions. The fabricated nanocomposites were initially cut into cylindrical pins of dimensions 8.5 mm diameter and 15 mm height using water jet machining. Different grades of emery sheets were used to smoothen the tip of the fabricated

pin. The counterpart, used to test the wear characteristics of the nanocomposites, was fabricated using hardened steel of EN31 grade having a diameter of 30 mm, thickness of 20 mm and surface finish of 0.1  $\mu\text{m}$ . The sliding speed was fixed at 0.1 m/sec and normal load at 5 N for all the fabricated polymer nanocomposites. Figure 9 shows the rate of coefficient of friction obtained during wear test for all the fabricated polymer nanocomposites. During wear test the incorporation of nanoparticles decreases the mass loss of all the fabricated nanocomposites. However, the friction coefficient of pure HDPE polymer (S7) was lower than that of nanocomposites incorporated with graphene particles (S3 and S6) and  $\text{Al}_2\text{O}_3$  (S1 and S4). The ease with which HDPE expands under dry sliding conditions, where heat generation is enormous makes it unsuitable for tribological applications. The frictional coefficient of the nanocomposites incorporated with MWCNT nanoparticles (S2 and S5) was lowest.

Figure 10(a-c) clearly indicates the pullout of particles in the wear track image. The wear track of HDPE/ $\text{Al}_2\text{O}_3$  specimen (Figure 10(b)) shows particle agglomeration and non-homogeneous mixing of  $\text{Al}_2\text{O}_3$  particles. The nanoceramic  $\text{Al}_2\text{O}_3$  particles act as an abrasive, leading to delamination and micro cracks, generating worn tracks on the fabricated composites. The wear track of HDPE/MWCNT nanocomposites (Figure 10(c)) was smoother as compared to other worn surfaces.

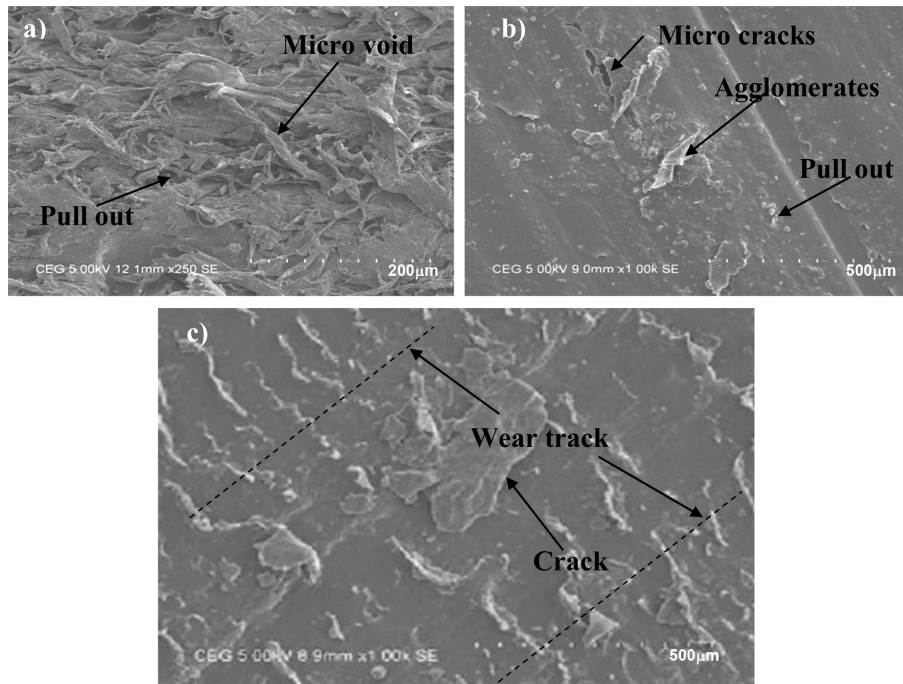


**Figure 10.** SEM images after wear of (a) HDPE/graphene; (b) HDPE/ $\text{Al}_2\text{O}_3$ ; (c) HDPE/MWCNT.

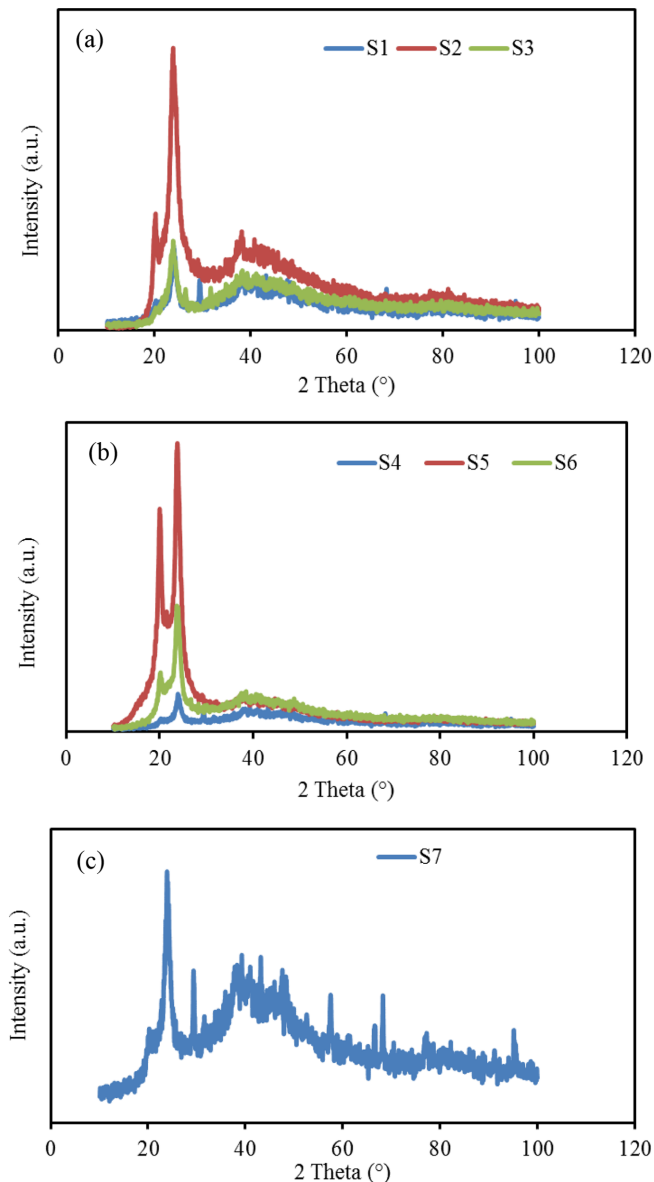


**Figure 11.** XRD patterns of (a) HDPE nanocomposites fabricated with rotational speed 800 rpm; (b) HDPE nanocomposites fabricated with rotational speed 1000 rpm; (c) pure HDPE.

Addition of MWCNT particles with HDPE improves its mechanical properties of HDPE including wear resistance. This can be attributed to the deep pinning of MWCNT particles within the HDPE matrix. During wear test these particles do not peel-off easily from the matrix. Moreover a thin carbon film formed out of MWCNT nanoparticles act as a lubricant during wear test thereby lowering the frictional coefficient of the fabricated nanocomposites. This leads to a lower mass loss of 0.00001 g.

**X-ray Diffraction of Fabricated Composites.** X-ray dif-

fraction plays a central role in identifying and characterizing solids. The nature of bonding and the working criteria for distinguishing the short-range and long-range order of crystalline arrangements from the amorphous substances are largely derived from X-ray diffraction and it thus remains a useful tool to obtain structural information.<sup>39</sup>

Figure 11(a-c) shows the X-ray diffraction (XRD) patterns of the fabricated HDPE polymer nanocomposites at two different conditions and pure HDPE. Pure HDPE exhibits a strong reflection peak at 23.95° followed by a less intensive peak at 40.57°. The HDPE/MWCNT nanocomposites (samples S5 and S2) fabricated at a rotational speed of 1000 rpm and 800 rpm exhibit a strong reflection peak at 23.89°. The results also show that the higher reflection peak for all the fabricated nanocomposites lie between 23.71° to 23.95°. Thus it is reasonable to assume that the morphology of all the fabricated nanocomposites show a homogeneous mixture of polymer matrix and reinforcements. The XRD pattern also shows that the addition of MWCNT/Al<sub>2</sub>O<sub>3</sub>/Graphene nanoparticles does not affect the original crystal structure of the HDPE matrix. Moreover the increase in the mechanical properties of the fabricated composites as compared to HDPE matrix without altering its crystal structure shows the effectiveness of the designed FSP tooling system. Out of all the fabricated nanocomposites MWCNT reinforced samples displayed the highest reflection peak in XRD pattern.

## Conclusions

In this study a newly developed friction stir processing tool and fixture was used to successfully fabricate HDPE/Al<sub>2</sub>O<sub>3</sub>, HDPE/MWCNT and HDPE/graphene nanocomposites. The new tooling system and fixture was highly efficient in the fabrication of defect free nanocomposites. The particle dispersion within the fabricated composites was remarkably good. Based on the study the following conclusions can be drawn.

- HDPE/Al<sub>2</sub>O<sub>3</sub>, HDPE/MWCNT and HDPE/graphene composites fabricated with a rotational speed of 1000 rpm and traverse feed of 15 mm/min has nearly 10% higher ultimate tensile strength, yield strength and percentage elongation as compared to the HDPE polymer.
- The enhanced mechanical properties of the fabricated composites confirms the effectiveness of the newly developed FSP tooling and fixture system as compared to the conventional FSP approach.
- The stress-strain graphs indicate that under all the con-

ditions HDPE/graphene nanocomposites have higher mechanical properties than the HDPE/Al<sub>2</sub>O<sub>3</sub> and HDPE/MWCNT nanocomposites.

- Pure HDPE, though has nearly 14.5% lower frictional coefficient than HDPE/graphene and HDPE/Al<sub>2</sub>O<sub>3</sub>, is unsuitable for tribological applications as it expands during dry sliding conditions.

- The friction coefficient of HDPE/graphene increases steadily when compared to the other samples owing to the pullout of graphene particles.

- The mass loss of HDPE//MWCNT (0.00001 g) worn surface was lower than the mass loss in the worn surfaces of other samples.

- The X-ray diffraction results show that the higher reflection peak for all the samples lie between 23.71° to 23.95°. This indicates that the crystal structure of HDPE matrix is not significantly altered by the addition of nanoparticles.

## References

1. M. Barmouz, J. Seyfi, M. K. B. Givi, I. Hejai, and S. M. Davachi, *Mater. Sci. Eng. A*, **528**, 3003 (2011).
2. A. O. Ogah and J. N. Afukwa, *Int. J. Engg. Manag. Sci.*, **3**, 85 (2012).
3. B. Chen, J. Wang, and F. Yan, *Tribol. Lett.*, **42**, 17 (2011).
4. N. Khare, P. K. Limaye, N. I. Soni, and R. J. Patel, *Wear*, **342-343**, 85 (2015).
5. J. H. Han, J. Zhang, P. F. Chu, A. Imani, and Z. Zhang, *Compos. Sci. Technol.*, **114**, 1 (2015).
6. H. Koike, K. Kida, K. Mizobe, X. Shi, S. Oyama, and Y. Kashima, *Tribol. Int.*, **90**, 77 (2015).
7. M. F. Diop, W. R. Burghardt, and J. M. Torkelson, *Polymer*, **55**, 4948 (2014).
8. F. Alam, A. Kumar, A. K. Patel, R. K. Sharma, and K. Balani, *JOM*, **67**, 688 (2015).
9. Q. Wang, Y. Wang, H. Wang, N. Fan, and F. Yan, *Tribol. Int.*, **104**, 73 (2016).
10. J. W. Lee, J. H. Kim, S. G. Ji, K. S. Kim, and Y. C. Kim, *Polym. Korea*, **39**, 572 (2015).
11. W. Y. Jung and J. I. Weon, *Polym. Korea*, **39**, 873 (2015).
12. S. M. Zebarjad and M. Noroozi, *Fiber Rein. Comp. Conference*, December 9-12 (2007).
13. V. N. Zhitomirsky, I. Grimberg, M. C. Joseph, R. L. Boxman, A. Matthews, and B. Z. Weiss, *Surf. Coat. Technol.*, **120-121**, 373 (1999).
14. A. S. Luyt, J. A. Molefi, and H. Krump, *Polym. Degrad. Stab.*, **91**, 1629 (2006).
15. S. Kanagaraj, F. R. Varanda, T. V. Zhiltsova, M. S. A. Oliveira, and J. A. O. Simoes, *Comp. Sci. Technol.*, **67**, 3071 (2007).
16. J. R. Lee, D. G. Lee, S. M. Hong, and H. J. Kang, *Polym. Korea*, **29**, 385 (2005).
17. J. C. Kim, J. H. Lee, and J. D. Nam, *Polym. Korea*, **27**, 275 (2003).
18. J. H. Kim and Y. S. Soh, *Polym. Korea*, **23**, 869 (1999).
19. C. Y. Chee, N. L. Song, L. C. Abdullah, Thomas S. Y. Choong, A. Ibrahim, and T. R. Chantara, *J. Nanomater.*, Article ID 215-978 (2012).
20. R. Sengupta, M. Bhattacharya, S. Bandyopadhyay, and A. K. Bhowmick, *Prog. Polym. Sci.*, **36**, 638 (2011).
21. A. Bhattacharyya, S. Chen, and M. Zhu, *eXPRESS Polym. Lett.*, **8**, 74 (2014).
22. Y. Lin, J. Jin, and M. Song, *J. Mater. Chem.*, **21**, 3455 (2011).
23. M. El Achaby and A. Qaiss, *Mater. Des.*, **44**, 81 (2013).
24. B. Arash, H. S. Park, and T. Rabczuk, *Composites Part B*, **80**, 92 (2015).
25. V. Kočović, S. Mitrović, G. Mihajlović, M. Mijatović, B. Bogdonavić, Đ. Vukelić, and B. Tadić, *Tribol. Ind.*, **37**, 434 (2015).
26. M. Puviyarasan and V. S. Senthil Kumar, *Arab. J. Sci. Eng.*, **40**, 1733 (2015).
27. M. Puviyarasan and V. S. Senthil Kumar, *J. Balkan. Tribol. Asso.*, **22**, 3994 (2016).
28. S. A. Hosseini, K. Ranjbar, R. Dehmlaei, and A. R. Amirani, *J. Alloys Comp. D*, **622**, 725 (2015).
29. T. Prakash, S. Sivasankaran, and P. Sasikumar, *Arab. J. Sci. Eng.*, **40**, 559 (2015).
30. M. K. Bilici, A. I. Yukler, and M. Kurtulmus, *Mater. Des.*, **32**, 4074 (2011).
31. M. K. Bilici and A. I. Yukler, *Mater. Des.*, **33**, 145 (2012).
32. A. Arici and T. Sinmaz, *J. Mater. Sci.*, **40**, 3313 (2005).
33. M. A. Rezugui, M. Ayadi, A. Cherouat, K. Hamrouni, A. Zghal, and S. Bejaoui, *EPJ Web Conf.*, **6**, 07003 (2010).
34. E. Azarsa and A. Mostafapour, *J. Manuf. Processes*, **15**, 682 (2013).
35. C. M. Rejil, I. Dinaharan, S. J. Vijay, and N. Murugan, *Mater. Sci. Eng. A*, **552**, 336 (2012).
36. I. A. Ovidko, *Rev. Adv. Mater. Sci.*, **34**, 19 (2013).
37. C. Lee, X. Wei, J. W. Kysar, and J. Hone, *Science*, **321**, 385 (2008).
38. I. A. Ovidko, *Rev. Adv. Mater. Sci.*, **34**, 1 (2013).
39. F. Chouit, O. Guellati, S. Boukhezar, A. Harat, M. Guerioune, and N. Badi, *Nanoscale Res. Lett.*, **9**, 288 (2014).